P AND S WAVE VELOCITY STRUCTURE OF THE CRUST AND UPPER MANTLE UNDER CHINA AND SURROUNDING AREAS FROM BODY AND SURFACE WAVE TOMOGRAPHY

M. Nafi Toksöz, Robert D. Van der Hilst, Youshun Sun, and Chang Li

Massachusetts Institute of Technology

Sponsored by Air Force Research Laboratory

Contract No. FA8718-04-C-0018

ABSTRACT

The objective of this project is to use a combination of travel-time and surface wave tomography to obtain compressional and shear wave velocity distributions in the crust and upper mantle under China and surrounding areas.

The first phase of the study is directed at producing a P-wave velocity model based on travel-time tomography. Travel data from the Annual Bulletin of Chinese Earthquakes (ABCE) and the International Seismological Centre (ISC/EHB) are used. The tomographic inversion is carried out in two steps. First, the regional travel-time data from ABCE is used to obtain the crust/uppermost mantle (0 to 100 km depth) velocity model. A total of 345,000 P-wave regional travel times are used for the tomography. Two discontinuities (Conrad and Moho) are allowed in the inversion. The tomographic model provides three-dimensional (3-D) velocities in the crust and uppermost mantle, depth to the Moho, and detailed P_n velocities.

To extend the model deeper into the mantle through the upper mantle transition zone, ISC/EHB data for P and p^P phases are combined with the ABCE data. To counteract the "smearing effect," the crust and upper mantle velocity structure derived from regional travel times, as described above, are used for teleseismic tomography. A variable grid method based on ray density is used in the inversion. A 3-D P-wave velocity model extending to 1700 km depth is obtained.

The combined regional teleseismic tomography provides a high-resolution, 3-D P-wave velocity model for the crust, upper mantle, and transition zone. The crustal models correlate well with geologic and tectonic features. The mantle models show the images of current and past subduction zones. A surprising result is that the "roots" of some geologic features, such as the Sichuan Basin and Ordos Plateau, extend deep into the upper mantle.

OBJECTIVES

The primary goal of this project is to obtain compressional and shear wave velocity distributions in the crust and upper mantle under China and surrounding areas using a combination of travel-time and surface wave tomography. The first phase of the study is directed at producing a P-wave velocity model based on travel-time tomography.

RESEARCH ACCOMPLISHED

Introduction

China and the surrounding area is a seismically active and geologically complex region (Figures 1 and 2). More than 500 earthquakes with magnitudes (M) greater than 6.0 occurred in this region between January 1978 and May 2004 (Figure 1). From a geological point of view, there are four Precambrian platforms (Figure 1) in China and the surrounding area: the North China Block, the South China Block, the Tarim Basin and the Indochina Block. There are distinct basins (e.g., Sichuan and Ordos) filled with deep sediment.

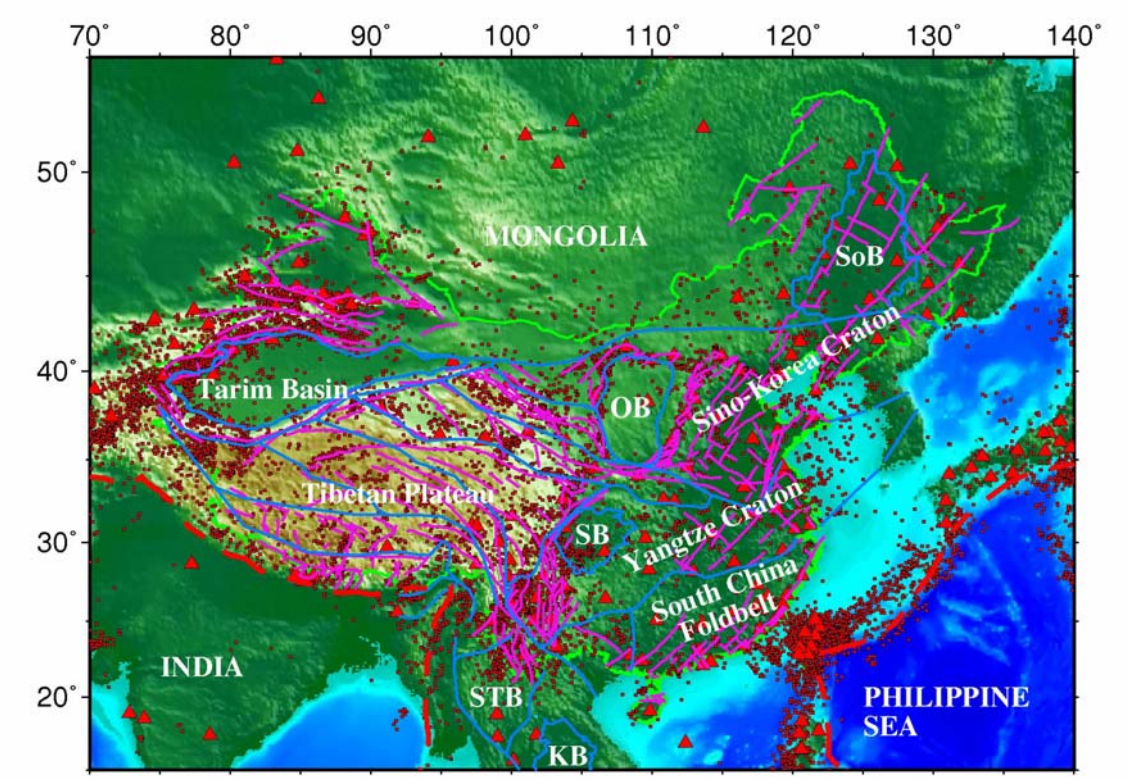

Figure 1. Locations of 512 earthquakes (M > 6.0 from January 1978 to May 2004), 220 stations, active faults and major tectonic boundaries in China and the surrounding area. Earthquake epicenters are shown in red dots and stations are shown in red triangles. The yellow line shows the boundary of China. Active faults in the China area are shown in purple lines and tectonic sutures are shown in blue lines, where SoB=Songliao Basin, OB=Ordos Basin, SB=Sichuan Basin, KB=Khorat Basin, STB=Shan Thai Block, and IB=Indochina Block.

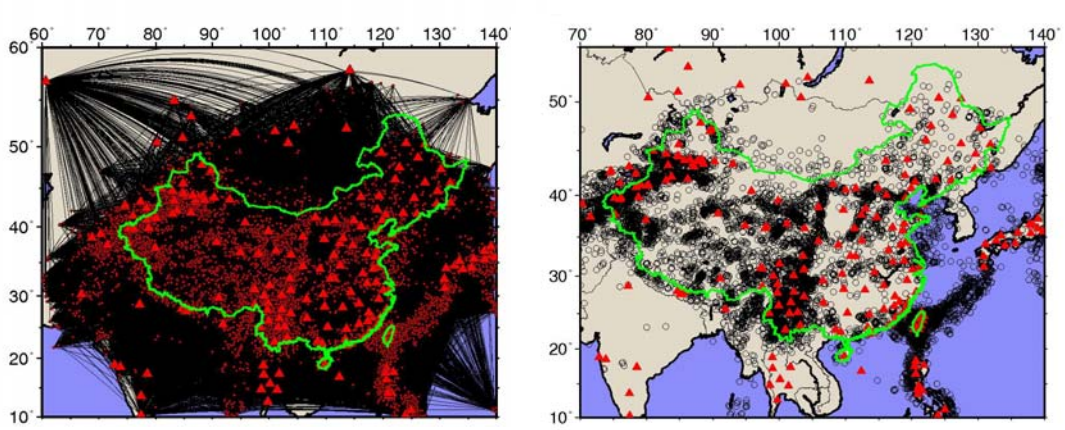

Figure 2. Left: Locations of 25,000 earthquakes, 220 stations, and 500,000 ray paths in China and the surrounding area. Earthquake epicenters are shown in black circles and stations are shown in red triangles. The green line shows the boundary of China. Right: Distribution of seismic stations and epicenters of selected earthquakes used in this study. A total of 16,572 events M 3.0 and greater are selected and plotted in black circles. All 220 stations are used and plotted in red triangles.

A high-resolution 3-D velocity model of China is necessary to provide accurate travel-times for reliable determination of earthquake locations. Large-scale models obtained by the teleseismic tomography technique generally cannot resolve vertical variations in the shallow structure. Regional models can be combined in order to cover a large area, but such models cannot guarantee smooth and consistent transitions between different regions. During the last several years, there have been many digital seismic stations installed in the China area (Figure 1). The large database of high-quality recorded arrival times provides an unprecedented opportunity to determine a detailed 3-D crustal structure under the region. Therefore, we introduce a method that constructs 3-D P-velocity models for the whole China area based on observed travel-time data.

The available P-wave velocity models of the crust and upper mantle in China and the surrounding area have been obtained using a variety of approaches. Some global models, such as CUB 1.0 (Shapiro and Ritzwoller, 2002) and the Science Application International Corporation 1° x 1° model (Stevens et al., 2001), were constructed from group and phase velocity dispersion measurements of surface waves. The global model CRUST 2.0 (Laske et al., 2001) was constructed from seismic refraction data and developed from the CRUST 5.1 model (Mooney, 1998) and a 1° x 1° sediment map (Laske and Masters, 1997). Although CRUST 2.0 was created by tomographic inversion, there are too few deep seismic soundings (DSSs) to provide enough refraction data for a detailed model. Regional models were constructed by Pn and/or Sn tomography (Ritzwoller et al., 2002; Hearn et al., 2004; Liang et al., 2004; Pei et al., 2004a), from surface waves (Wu et al., 1997, Lebedev and Nolet, 2003; Huang et al., 2003; Song et al.,1991; Zhu et al., 2002), and from P-wave travel-time tomography (Liu et al.,1990). The model of Liu et al. (1990) was constructed by regional and teleseismic tomography. The maximum and minimum grid spacings in the model of Liu et al. (1990) are 5° x 5° and 2° x 2°, respectively, in the horizontal direction, and 300 km and 45 km in the vertical direction. This model does not have the details for local and regional travel-time calculations and precise earthquake locations.

P-wave tomography has been performed in several local regions in China (Xu et al., 2002; Huang et al., 2002; Yu et al., 2003; Huang and Zhao, 2004; Sun and Liu, 1995; Zhu et al., 1990; Pei et al., 2004b). These models show detailed crustal structures only in a few regions. A detailed map for the whole China area remains to be developed.

In this study, we carry out the 3-D velocity tomography in two steps. First, we use the ABCE regional travel-time data to obtain the crust/uppermost mantle (0–100 km depth) velocity structure. Then, we extend the model deeper into the mantle through the transition zone using the ISC/EHB and ABCE data, and the shallow (1–100 km) velocity model from the first step.

Regional Travel-Time Data and 3-D Tomography

In this work, we use the earthquake phase data (first P-wave arrivals) from January 1990 to December 2003, found in the ABCE (IG-CSB, 1990-2003). There are 25,000 earthquakes, 220 stations, and 500,000 ray paths in China and the surrounding area in this database. Figure 2 shows earthquake epicenters, the stations, and the ray paths. We also incorporated special data such as 129 earthquakes with high-quality records and three quarry blast events (ground-truth events) from the Sichuan Province.

The study area is divided into parallelepipeds with a spatial size of 10 km x 10 km x 2 km. Among the earthquakes within each block, we select the event with the greatest number of first P-wave arrivals and the smallest hypocentral location uncertainty. As a result, our final dataset contains 16,000 events with more than 300, 000 ray paths. The ray coverage has a better (more uniform) distribution in the study area (Figure 2), thus it is more appropriate for tomographic study than the original dataset. Since most aftershocks occur in similar locations with smaller magnitudes and tend to produce larger reading errors for the phase arrivals than the main shocks, the final dataset contains the least number of aftershocks possible.

The starting model for the tomography is a 3-D model created with the adaptive moving window (AMW) method (Sun et al., 2004). The model assumes a layered crust and a one-layer uppermost mantle at each one degree intersection of longitude and latitude. The thickness and P-wave velocity of each layer are found from the observed travel-times. These 1° x 1° velocity profiles are quilted together with a suitable smoothing to obtain the starting model for the 3-D tomography. The model includes discontinuities such as the Conrad and the Moho. Although there is general consensus on the Moho (China Seismological Bureau, 1986; Zhang, 1998; Li et al., 2001; Hearn et al., 2004; Sun et al., 2004), the Conrad discontinuity is clear only in some regions of the study area, and therefore we only incorporate the Moho discontinuity in this study. Figure 3 shows the geometry of the Moho discontinuity as input into the 3-D tomography.

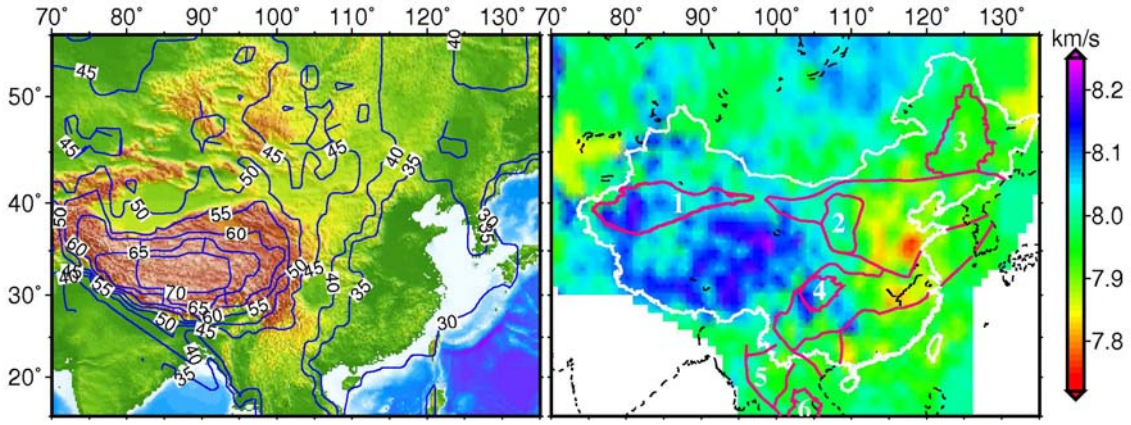

Figure 3. Depth distribution of the Moho discontinuities (left) and Pn velocities (right) in the present study area obtained by inverting the 1-D layered models from first arrivals of P-wave travel-time (Sun et al. 2004). The Moho depths are shown in contours. 1=Tarim Basin, 2=Ordos Basin, 3=Songliao Basin, 4=Sichuan Basin, 5=Shan Thai Block, and 6=Khorat Basin.

We used a modified version of the tomographic method of Zhao et al. (1992) to invert for the crustal and uppermost mantle velocity structure in China and the surrounding area. Zhao's method, described in detail in several papers (Zhao et al., 1992, 1994; Zhao, 2001), allows 3-D velocity variations everywhere in the model and can accommodate velocity discontinuities. The velocity structure is discretized using a 3-D grid. The velocity perturbation at each point is calculated by linearly interpolating the velocity perturbations at the eight surrounding (adjacent) grid nodes. Velocity perturbations at grid nodes are the unknown parameters for the inversion procedure. To calculate travel-times and ray paths accurately and rapidly, an efficient 3-D ray-tracing technique is employed to iteratively use the pseudo-bending technique (Um and Thurber, 1987) and Snell's law. Station

elevations and the sediment layers are taken into account in the ray tracing. The LSQR algorithm (Paige and Saunders, 1982) with a damping regularization is used to solve the large and sparse system of equations. The nonlinear tomographic problem is solved by iteratively conducting linear inversions.

Crust and Uppermost Mantle Velocity Models

The 3-D P-wave velocity models are shown at constant depths in Figure 4. At a depth of 40 km, low velocity (low-V) zones are visible in the western part of China, and high-velocity (high-V) zones exist in the eastern part. A clear dividing line appears around 105°E separating the east and west seismic zones in mainland China. At a depth of 60 km, the Tibetan plateau's thick crust is clearly outlined as a low-V zone. At a depth of 80 km, the root of the Tibetan plateau disappears, and high-V zones appear in the west and south part of the Tibetan Plateau. There are a few low-V zones sandwiched between the high-V zones. The deeper velocity slices (60 km and 80 km) with scattered low-V zones in eastern China indicate the presence of tectonic extension in the area. These results are consistent with those obtained by a joint inversion of the DSS data from multiple profiles (Li et al., 2001).

The Pn velocity image remains basically unchanged from the starting model. It has a high resolution in the whole study area (Figure 3). Pn velocities are low at the center of the Songliao Basin, but high under most of the Tarim Basin, the Sichuan Basin, and the Ordos Basin. This result is generally consistent with the recent Pn tomography by Pei et al. (2004a), Liang et al. (2004), and Hearn et al. (2004).

Velocity changes are visible across some of the fault zones such as the Sanjiang Folding Belt. Such a feature is visible from a depth of 10 km to a depth of 30 km, suggesting that some of the faults may have cut through the crust and reached to the middle or lower crust. No velocity contrast is visible across most of the faults, particularly in the middle to lower crust. Some features are associated with the basins.

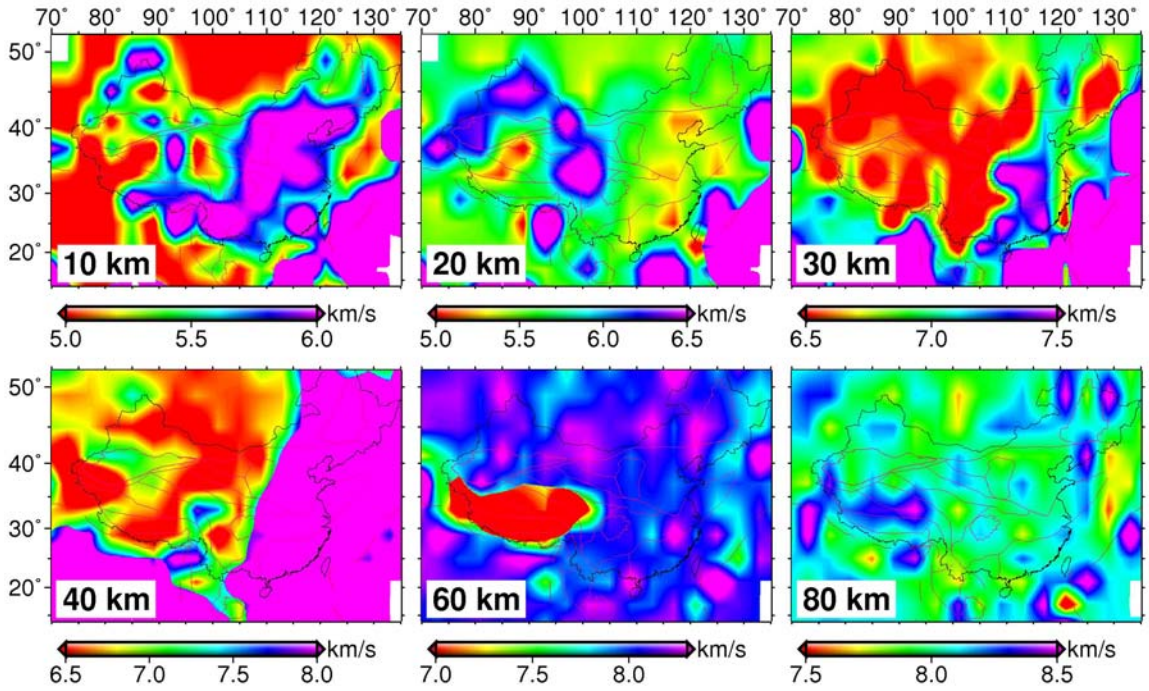

Figure 4. P-wave velocity image at each depth slice. The depth of each layer is shown at the lower-left corner of each map.

Validation with Ground Truth (GT) events

We test our 3-D model by relocating the GT events and comparing the results with known locations. Eleven GT events are the nuclear explosions in northwestern China from 1990 to 1996, recorded by stations in China and the surrounding area. Only P-wave travel-times are available in the dataset.

The GT events are closely clustered. Table 1 shows the parameters for these nuclear explosions (Sun, 2005). With our new P-wave velocity model for the crust and upper mantle in China and the surrounding area, we relocate the GT events using travel-time data recorded at stations within 20° epicentral distance. The relocation errors are also listed in Table 1. The three columns under "Error" are the hypocentral difference in kilometers between the reference hypocenters and relocations using the new 3-D P-wave model, 1-D average China model obtained from the 3-D model, and the AK135 global model.

The averaged hypocentral error of relocation is only 0.9 km with a standard deviation of 0.3 km for the new 3-D P-wave model. The mean hypocentral misfit is about 10 km if the averaged 1-D velocity in China is used, and about 20 km if the global AK135 model is used. Even though the GT events are located in northwestern China and most stations distributed in southern and eastern China, the small relocation errors clearly suggest that an accurate P-wave velocity model gives good event locations with limited azimuthal coverage.

Table 1: The eleven GT events in northwest China. The relocation errors (hypocentral) are listed in km. Events are relocated using our new P-wave model, the averaged 1-D model in China and the surrounding area, and the standard AK135 (global).

Event No.	Date (Y/M/D)	Time (H/M/S)	Latitude (degree)	Longitude (degree)	Error (km)		
					3D	1D	AK135
1	1990/05/06	07:59:59.25	41.5618	88.7183	0.4	6.2	18.9
2	1990/08/16	04:59:59.26	41.5392	88.7445	1.2	9.5	23.0
3	1992/05/21	04:59:59.06	41.5419	88.7678	0.8	8.7	18.4
4	1992/09/25	08:00:00.02	41.7167	88.3767	1.3	9.1	17.8
5	1993/10/05	01:59:57.92	41.5922	88.7035	1.1	9.3	19.1
6	1994/06/10	06:25:59.46	41.5271	88.7074	0.9	8.1	18.4
7	1994/10/07	03:25:59.44	41.5741	88.7256	1.1	7.7	19.6
8	1995/05/15	04:05:59.38	41.5545	88.7516	0.8	8.8	24.9
9	1995/08/17	00:59:59.35	41.5402	88.7533	0.7	9.2	18.8
10	1996/06/08	02:55:59.37	41.5780	88.6875	1.0	9.3	20.1
11	1996/07/29	01:48:59.62	41.7162	88.3757	0.6	8.4	21.5

Extension of P-wave Velocity Models into the Mantle

To extend the velocity models into the mantle, we add the teleseismic travel-time data. To minimize the "smearing effect" of the shallow structure or teleseismic tomography, we constrain the uppermost (top 100 km) of the model with that obtained from regional data as described in sections 2 and 3. The 1964-2004 ISC/EHB regional/teleseismic database includes 9.4 million travel-times for P, p^P, and PP phases (Li et al. 2005). For the tomographic inversion we use an adaptive parameterization of the grid based on ray sampling density, and iterative LSQR with norm and gradient damping (Li et al., 2005).

Examples of velocity cross sections for shallow and deep structure are shown in Figures 5 and 6, respectively. A continuum of lithospheric and mantle velocity structure provides the means for calculating accurate travel-times and for understanding the lithospheric mantle geodynamic processes.

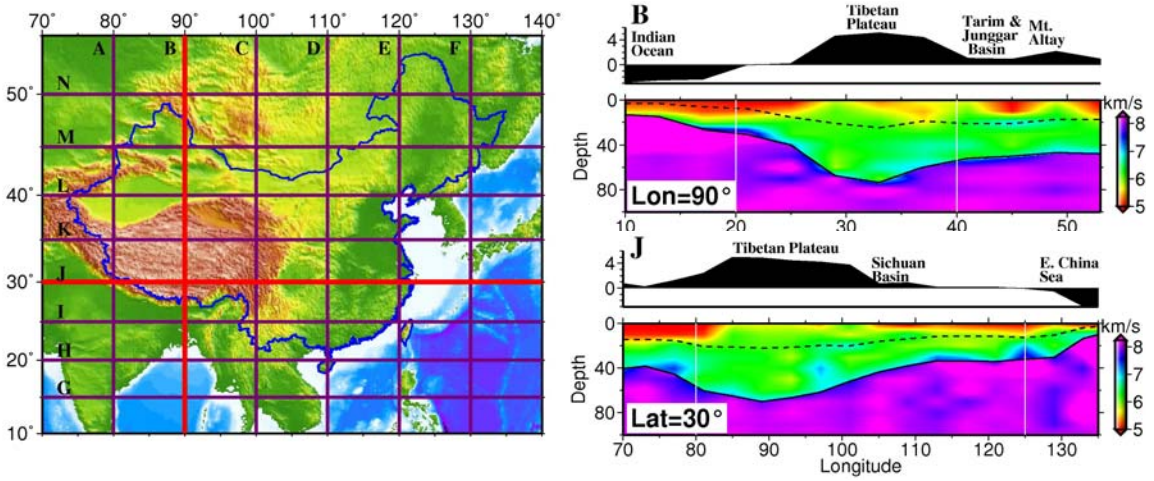

Figure 5. Vertical velocity profiles (right) of the crust and uppermost mantle. The selected profile locations are shown on the left.

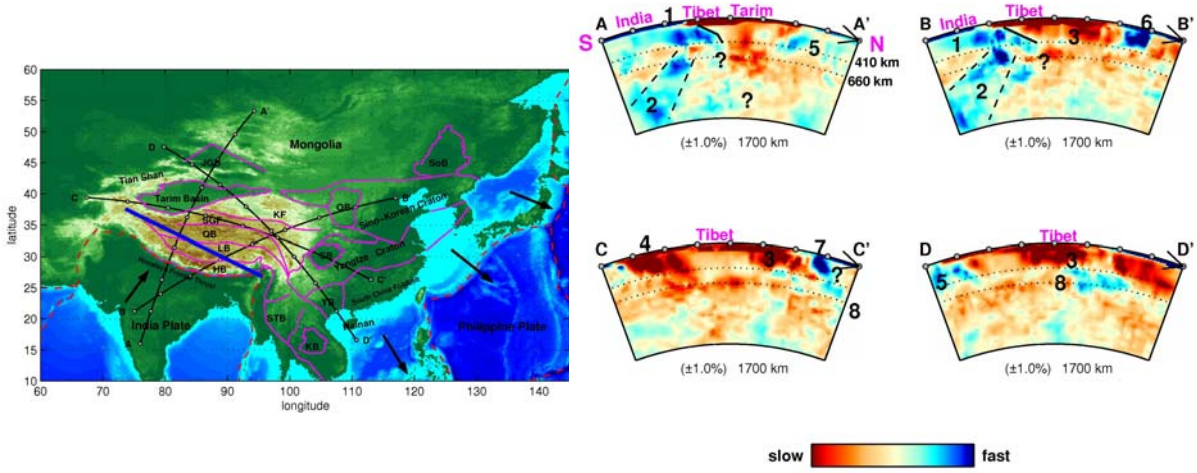

Figure 6. Vertical cross sections (right) of velocity image down to the mantle. The cross section locations are shown on the left.

CONCLUSIONS

Strong P-wave velocity variations of more than 10% found in the study area indicate the existence of significant structural heterogeneities in the crust and uppermost mantle in this region. The velocity models show the following features.

1. The seismic velocity images are characterized by block structures corresponding to geological features bounded by large fault zones. This region consists of a few geological structures: the North China Block including Songliao Basin, the South China Block, the Sichuan Basin, the Tarim Basin, and the Tianshan area. Those areas exhibit different patterns of velocity distribution in the tomographic images. The trend of velocity anomalies is consistent with the trend of regional tectonics.

2. A clear dividing line along the 105° parallel separates China into a low-V zone in the west and a high-V zone in the east at a depth of 40 km.

3. Our tomographic imaging has revealed significant velocity heterogeneities in the middle and lower crust.

4. Pn velocities are high under southern and eastern Tibet and under the Sichuan and Ordos basins.

The deeper velocity profiles show evidence of current and past subduction zones and other geodynamic processes. A surprising result is that the "roots" of some geologic features, such as the Sichuan Basin and Ordos Plateau, extend deep into the upper mantle.

REFERENCES

China Seismological Bureau, (1986), *Findings of Exploring the Crust and Upper Mantle Structure of China. Seismological Press,* 407 pp., Beijing (in Chinese).

Hearn, T. M., S. Wang, J. F. Ni, Z. Xu, Y. Yu, and X. Zhang, (2004), Uppermost mantle velocities beneath China and surrounding regions, *J. Geophys. Res. 109*, doi:10.1029/2003JB002874.

Huang, J., D. Zhao, and S. Zheng, (2002), Lithospheric structure and its relationship to seismic and volcanic activity in southwest China, *J. Geophys. Res. 107*, doi:10.1029/2000JB000137.

Huang, J., and D. Zhao, (2004), Crustal heterogeneity and seismotectonics of the Chinese capital region. *Tectonophysics, 385*, 159-180.

Huang, Z., W. Su, Y. Peng, Y. Zheng, and H. Li, (2003), Rayleigh wave tomography of China and adjacent regions, *J. Geophys. Res. 108*, doi 10.1029/2001JB001696.

Institute of Geophysics, China Seismological Bureau (IG-CSB), (1990-2003), *Annual Bulletin of Chinese Earthquakes (ABCE),* Seismological Publishing House, Beijing.

Laske, G., and G. Masters, (1997), A global digital map of sediments thickness (abstract), *EOS 78*, F483.

Laske, G., G. Masters, and C. Reif, (2001), CRUST 2.0: a new global crustal model at 2x2 degrees, http://mahi.ucsd.edu/Gabi/rem.dir/crust/crust2.html (last accessed July 2005).

Lebedev, S., and G. Nolet, (2003), Upper mantle beneath southeast Asia from S velocity tomography, *J. Geophys. Res. 108*, doi 10.1029/2000JB000073.

Li, C., R. van der Hilst, and M. N. Toksoz, (2005), Constraining P-wave velocity variation in the upper mantle beneath Southeast Asia, Submitted to PEPI.

Li, S., X. Zhang, and Z. Song, (2001), Three-dimensional crustal structure of the Capital area obtained by a joint inversion of deep seismic sounding data from multiple profiles, *Acta Geophys. Sin. 44,* 360-368 (in Chinese).

Liang, C., X. Song, and J. Huang, (2004), Tomographic inversion of Pn traveltimes in China, J. Geophys.Res. 109, B11304, doi:10.1029/2003JB002789.

Liu, F. T., H. Wu, J. H. Liu, G. Hu, Q. Li, and K. X. Qu, (1990), 3-D velocity images beneath the Chinese continent and adjacent regions, *Geophys. J. Int. 101*, 379-394.

Mooney, W. D., (1998), CRUST 5.1: a global crustal model at 5° x 5°, *J. Geophys. Res. 103*, 727-747.

Paige, C., and M. Saunders, (1982), LSQR: An algorithm for sparse linear equations and sparse least squares, ACM Trans. *Math. Software, 8*, 471.

Pei, S., Z. Xu, and S. Wang, (2004a), Discussion on origin of Pn velocity variation in China and adjacent region, *Acta Seismol. Sin. 26*, 1-10 (in Chinese).

Pei, S., Y. Chen, D. Zhao, A. Yin, J. Ning, and X. Chen, (2004b), Tomographic structure of east Asia and its geodynamic implication, Submitted to *J. Geophys. Res.*

Ritzwoller, M. H., M. P. Barmin, A. Villasenor, A. L. Levshin, and E. R. Engdahl, (2002), Pn and Sn tomography across Eurasia to improve regional seismic event locations, *Tectonophysics 358*, 39-55.

Shapiro, N. M., and M. H. Ritzwoller, (2002), Monte Carlo inversion for a global shear velocity model of the crust and upper mantle, *Geophys. J. Int. 151*, 88-105.

Song, Z. H., C. Q. An, G. Y. Chen, L. H. Chen, Z. Zhuang, Z. W. Fu, and J. F. Hu, (1991), Study on 3-D velocity structure and anisotropy beneath west China from the Love wave dispersion, *Acta Geophys. Sin. 34*, 694-707 (in Chinese).

Stevens, J. L., D. A. Adams, and G. E. Baker, (2001), Improved surface wave detection and measurement using phase-matched filtering with a global one-degree dispersion model, in *Proceedings of 23rd Seismic Research Review: Worldwide Monitoring of Nuclear Explosions,* LA-UR-01-4454, pp. 420-430.

Sun, Y., (2005), P- and S-wave tomography of the crust and uppermost mantle in China and surrounding areas, Ph.D. Thesis, Massachusetts Institute of Technology, Cambridge, Massachusetts.

Sun, R., and F. Liu, (1995), Crust structure and strong earthquakes in Beijing, Tianjin and Tanshan area, I. P wave velocity structure, *Acta Geophys. Sin. 38*, 599-607 (in Chinese).

Sun, Y., X. Li, S. Kuleli, F. D. Morgan, and M. N. Toksöz, (2004), Adaptive moving window method for 3-D P-velocity tomography and its application in China, *Bull. Seism. Soc. Am. 94*, 740-746.

Um, J., and C. Thurber, (1987), A fast algorithm for two-point seismic ray tracing, *Bull. Seism. Soc. Am. 77*, 972-986.

Wu, F. T., A. L. Levshin, and V. M. Kozhevnikov, (1997), Rayleigh wave group velocity tomography of Siberia, China, and vicinity, *Pure Appl. Geophys. 149,* 447-473.

Xu, Y., F. Liu, J. Liu, and H. Chen, (2002), Crust and upper mantle structure beneath western China from P wave travel-time tomography, *J. Geophys. Res., 107*, doi 10.1029/2001JB000402.

Yu, X., Y. Chen, and P. Wang, (2003), Three-dimensional P wave velocity structure in Beijing-Tianjin-Tangshan area, *Acta Seismol. Sin. 25,* 1-14.

Zhang, X., (1998), *Study of the Crust and Upper Mantle Structure in and Around the Zhangjiakou-Bohai Seismic Belt.* Active Fault Research (6), Seismological Press, Beijing.

Zhao, D., (2001), New advances of seismic tomography and its applications to subduction zones and earthquake fault zones: A review, *The Island Arc, 10*, 68-84.

Zhao, D., A. Hasegawa, and S. Horiuchi, (1992), Tomographic imaging of P and S wave velocity structure beneath northeastern Japan, *J. Geophys. Res., 97,* 19909-19928.

Zhao, D., A. Hasegawa, and H. Kanamori, (1994), Deep structure of Japan subduction zone as derived from local, regional and teleseismic events, *J. Geophys. Res., 99*, 223122329.

Zhu, J., J. Cao, X. Cai, Z. Yan, and X. Cao, (2002), High resolution surface wave tomography in east Asia and west pacific marginal sea, *Chinese J. Geophys., 45*, 679-698.

Zhu, L., R. Zeng, and F. Liu, (1990), 3-D P wave velocity structure under the Beijing network area, *Acta Geophys. Sin.,* 33, 267-277 (in Chinese).